Supplemental Material

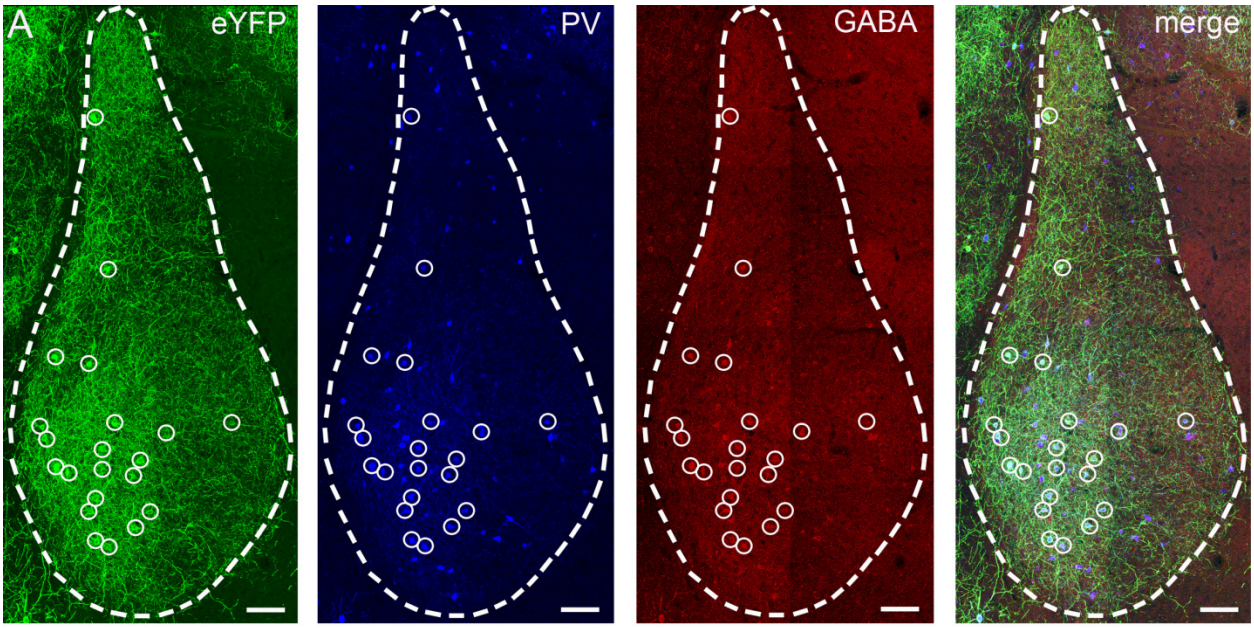

B

	Animal # 1	2	3	4	Total
PV+	118	216	176	139	649
PV+/GABA+	78	111	113	66	368
YFP+	41	69	42	32	184
YFP+/PV+	41	67	40	31	179
YFP+/GABA+	39	61	41	29	170
YFP+/PV+/GABA+	39	60	39	29	167

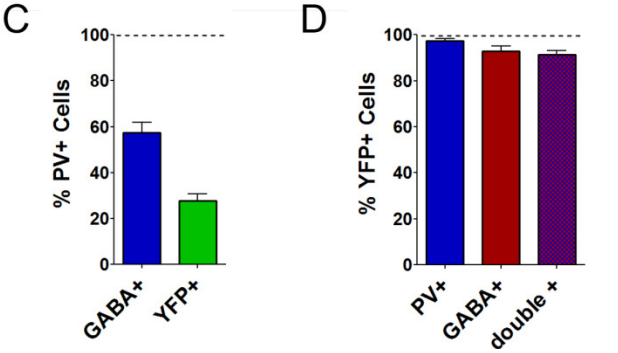

Figure S1. ***PV-IRES-Cre recombination throughout the basolateral amygdala***, related to Figure 1. PV-IRES-Cre mice were crossed to R26-stop-eYFP reporter mice to express eYFP specifically in PV-INs. **A.** Double immunofluorescence staining with antibodies against PV (blue) and GABA (red) show that Cre-dependent recombination is restricted to GABAergic PV-INs. Scales = 100 µm. **B.** Cell counts from 50 µm thick coronal sections from males at postnatal day 35. n = 4 animals, 3 sections/animal. **C.** Corresponding to a previous investigation (McDonald and Mascagni, 2001), approximately 60% of PV+ neurons coexpressed GABA in the basolateral amygdala. Approximately 30% of PV+ neurons exhibited recombination in this mouse line. **D.** The overwhelming majority of eYFP+ cells (> 90%) were GABAergic PV-INs. Data presented as mean ± SEM.

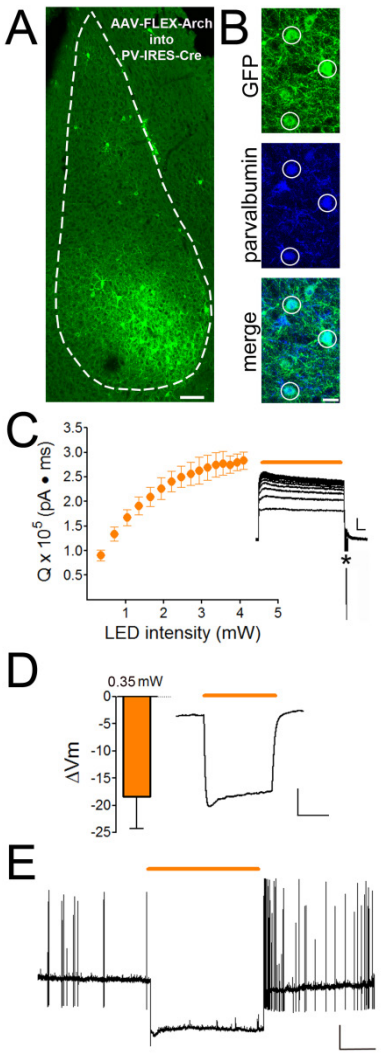

Figure S2. ***Validation of Arch3.0 in PV-INs***, related to Figure 2. **A.** AAV-Flex-Arch-GFP was injected into the basolateral amygdala of PV-IRES-Cre mice for optogenetic-assisted slice electrophysiology, scale = 100 μm. **B.** Immunofluorescence staining confirmed that GFP (green) was exclusively expressed in PV-positive neurons (blue), scale = 25 μm. **C.** Whole-cell voltage clamp recordings from GFP-positive PV-INs revealed the input-output relationship of LED intensity (λ = 590 nm) and eArch3.0 conductance. Representative traces are shown in the inset, scale = 50 pA x 100 ms. * in inset indicates rebound action currents, which have been shortened for clarity. **D.** Current clamp recordings confirmed the hyperpolarizing effect of 590 nm light. A representative trace is shown in the inset, scale = 20 mV x 250 ms. n = 4 (3). **E.** Light-induced hyperpolarization of Arch3.0-expressing PV-INs was sufficient to silence action potential generation. Scale = 15 mV x 15 ms. Data presented as mean ± SEM.

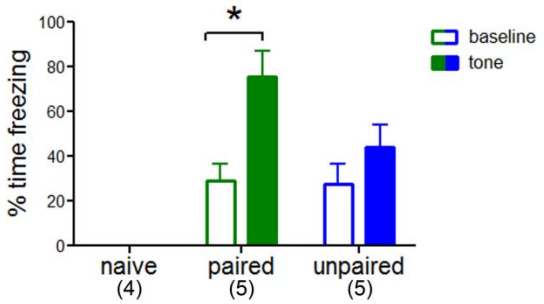

Figure S3. ***Validation of behavioral paradigm***, related to Figures 3-7**.** PV-IRES-Cre x R26-stop-eYFP mice underwent paired or unpaired auditory fear conditioning. Fear memory retrieval was assessed 24 hours later with 4 presentations of the CS, at the time point when animals were sacrificed for electrophysiological recordings. Only animals in the paired training paradigm exhibited increased freezing to the CS compared to baseline. n/group indicated on bar histogram. Two-way ANOVA; main effect of group, $F_{(2,22)} = 47.75$, $p < 0.0001$; main effect of CS, $F_{(1,22)} = 11.75$, $p < 0.007$; interaction, $F_{(2,22)} = 9.84$, $p < 0.04$. Holm-Bonferroni post-test, *$p < 0.01$. Data presented as mean ± SEM.

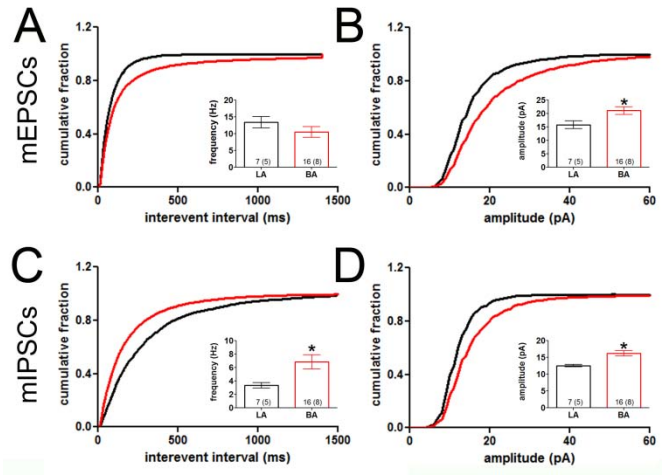

Figure S4. ***Differences in mEPSC and mIPSC frequency and amplitude in LA versus BA PV-INs***, related to Figure 3. mEPSCs and mIPSCs were isolated in PV-INs by clamping membrane potential at -60 mV and 0 mV, respectively, in the presence of a low chloride cesium internal solution. No difference in frequency (**A,** $t_{(15)} = 1.23$, $p = 0.24$) but increased amplitude (**B,** $t_{(15)} = 2.58$, $p = 0.02$) of mEPSCs was observed in the BA compared to LA of naïve animals. Both the frequency (**C**, $t_{(18)} = 3.13$, $p = 0.006$) and amplitude (**D**, $t_{(20)} = 4.074$, $p = 0.0006$) of mIPSCs was increased in the BA compared to LA of naïve animals. n/group indicated on bar histogram. Independent samples t-tests. Data presented as mean ± SEM.

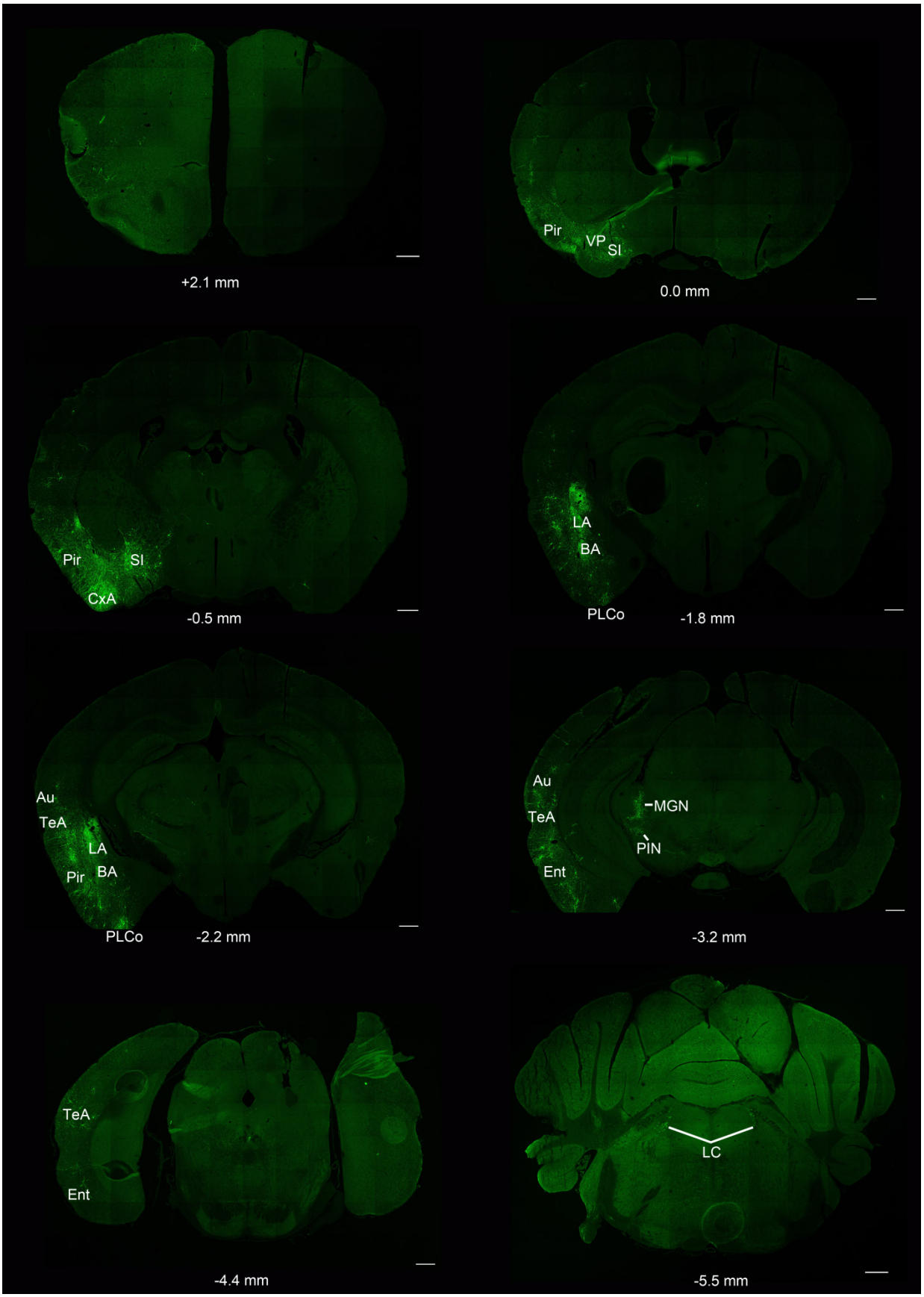
+2.1 mm
Pir
VP
SI
0.0 mm
Pir
SI
CxA
-0.5 mm
LA
BA
PLCo
-1.8 mm
Au
TeA
LA
Pir
BA
PLCo
-2.2 mm
Au
TeA
MGN
PIN
Ent
-3.2 mm
TeA
Ent
-4.4 mm
LC
-5.5 mm

Figure S5. ***Long-range innervation of amygdala PV-INs***, related to Figure 5. Four adult PV-IRES-Cre mice received unilateral basolateral amygdala infusions of an AAV encoding the conditional TVA receptor (AAV8-EF1a-FLEX-TVA-mCherry) and the rabies glycoprotein (AAV8-CA-FLEX-RG), followed by infusion of EnvA G-deleted Rabies-eGFP three weeks later. Mice were sacrificed by perfusion one week later, and GFP expression throughout the entire rostral-caudal axis of the brain was amplified with an anti-GFP antibody (green). Brain regions that were labeled in all 4 animals included the piriform (Pir) cortex, primary (Au) and secondary (TeA, temporal association cortex) auditory cortex, entorhinal (Ent) cortex, basal forebrain (VP, ventral pallidum; SI, substantia innominata), cortex-amygdala transition zone (CxA), posterolateral cortical amygdaloid nucleus (PLCo), sensory thalamus (MGN, medial geniculate nucleus; PIN, posterior intralaminar nucleus), and locus coeruleus (LC). Notably, the LC was the only bilaterally-projecting region. No GFP-labeled cells were observed in the medial prefrontal cortex of any animal. Scale bars = 500μm.

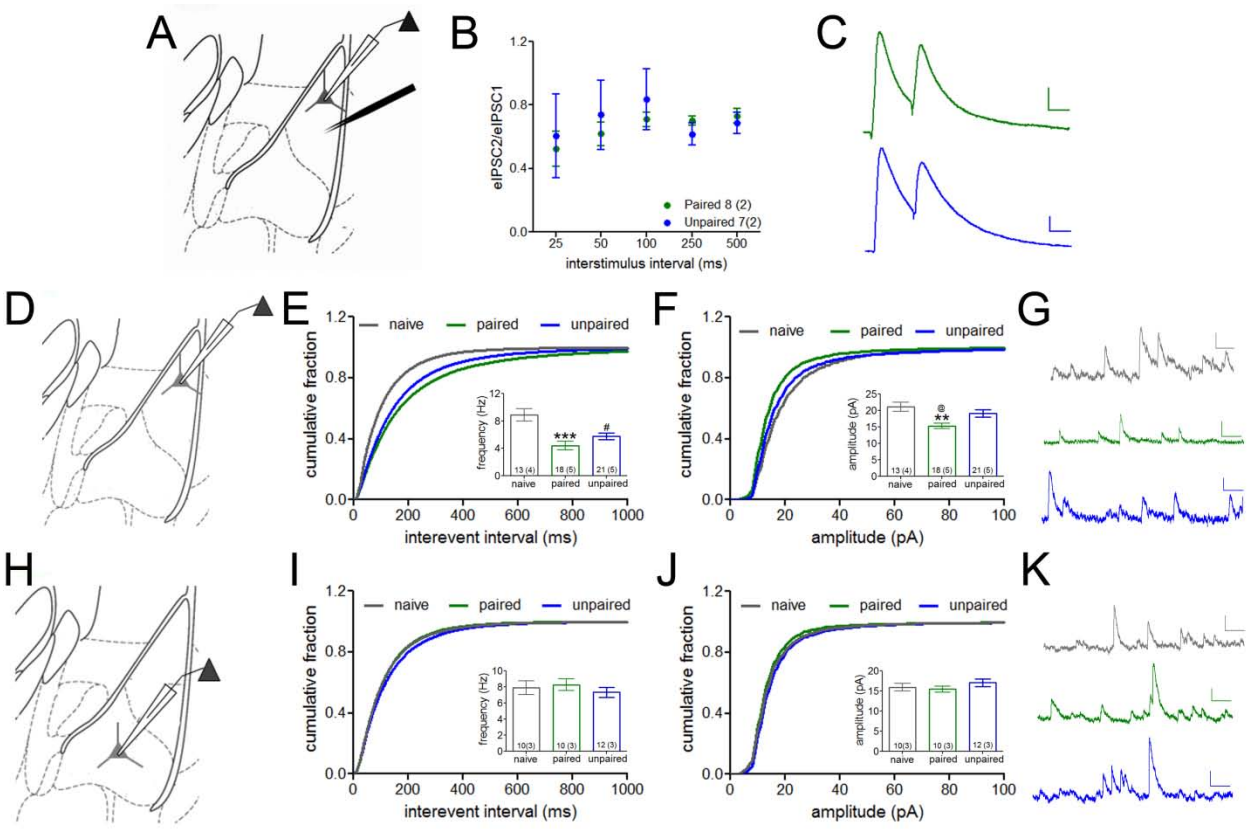

Figure S6. ***Reduced spontaneous inhibition onto principal neurons in LA but not BA after emotional learning***, related to Figure 6. **A.** In the presence of APV and CNQX, GABA release was evoked from a mixed population of local inhibitory neurons by paired-pulse stimulation during recording of IPSCs from LA PNs held at 0mV. **B.** PPR (eIPSC2/eIPSC1) did not differ between paired and unpaired animals. Representative traces in **C.** Scales = 50 pA x 25 ms. **D.** Recording configuration for E-G. **E.** The frequency of sIPSCs was reduced in paired and unpaired compared to naïve animals in LA. **F.** The amplitude of sIPSCs was reduced in paired compared to naïve and unpaired animals in LA. **G** Representative traces of LA sIPSCs. **H.** Recording configuration in I-K. **I.** The frequency of sIPSCs was not changed in BA. **J.** The amplitude of sIPSCs was not changed in BA. **K.** Representative traces of BA sIPSCs. Scales G,K = 20 pA x 100 ms. n/group indicated on bar histograms. One-way ANOVA followed by Fisher's LSD. * p < 0.05 naïve versus paired. @ p < 0.05 paired versus unpaired. # p < 0.05 naïve versus unpaired. One symbol p < 0.05, two symbols p < 0.005, three symbols, p < 0.0005. Data presented as mean ± SEM.

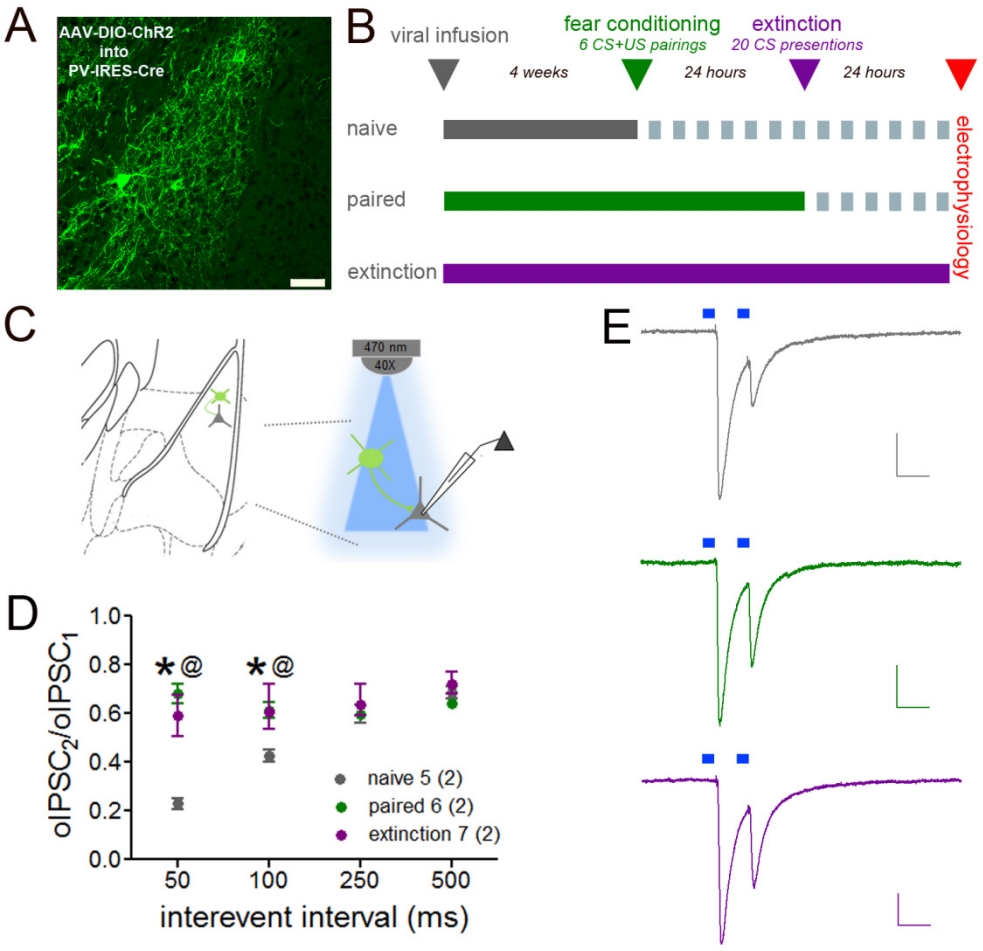

Figure S7. ***Learning-induced reduction of GABA release at PV-IN → principal neuron synapses is not reversed by extinction,*** related to Figure 6***.*** **A.** eYFP expression after viral infusion of AAV-DIO-ChR2 into the basolateral amygdala of PV-IRES-Cre mice. **B**. Experimental time line. Dashed gray line indicates the time point at which mice were sacrificed for whole-cell recordings. **C.** Experimental design. Paired pulse ratio of IPSCs evoked by blue light (λ = 470 nm) in LA principal neurons. **D.** PPR was increased in mice from the paired and extinction groups compared to the naïve group. **E.** Representative traces at the 50 ms interstimulus interval. Scales = 25 pA x 50 ms. n/group indicated on graph. Repeated-measures ANOVA; main effect of group, $F_{(2,45)} = 19.35$, $p < 0.0001$; main effect of interstimulus interval, $F_{(3, 45)} = 54.13$, $p < 0.0001$; interaction, $F_{(6,45)} = 35.57$, $p < 0.0001$. Holm-Bonferroni post-test, * p < 0.0001 paired versus naïve, @ p < 0.0001 extinction versus naïve. Data presented as mean ± SEM.

Supplemental Experimental Procedures.

Animals. All experiments were conducted on male animals 28-40 days of age. The following mouse lines were maintained on a C57Bl/6J background and obtained from Jackson Laboratories (Bar Harbor, ME, USA): C56Bl/6J (RRID:IMSR_JAX:000664), PV-IRES-Cre (RRID:IMSR_JAX:008069), R26-STOP-eYFP (RRID:IMSR_JAX:006148), and Rosa-CAG-LSL-tdTomato-WPRE (Ai9; RRID:IMSR_JAX:007909). Mice were housed 2-5 per cage with access to food and water *ad libitum* on a 12 hour light-dark cycle (lights on at 0700 hours). All experiments were approved in advance by the Institutional Care and Use Committee of the Icahn School of Medicine at Mount Sinai.

Viral targeting for electrophysiology. Viral constructs were purchased from the University of Pennsylvania Vector Core and included AAV1-EF1a-DIO-hChR2(H134R)-eYFP-WPRE (Addgene #20298), AAV1-CBA-Flex-Arch-GFP (Addgene #22222), and AAV1-CamKIIa-hChR2(H134R)-eYFP-WPRE (Addgene #26969P). Stereotaxic surgeries were conducted at 21-24 days of age. Animals were deeply anesthetized with a mixture of ketamine/xylazine (initial dose 100 mg/kg and 5 mg/kg, respectively) and mounted in a stereotaxic frame (Stoelting, Wood Dale, IL, USA). Viral constructs (0.3-1 µL) were bilaterally injected into the basolateral amygdala (AP -1.4, ML ±3.3, DV -5.0), temporal association cortex (AP -4.0, ML ±4.0, DV -3.5), and medial geniculate nucleus (AP -3.2, ML ±1.8, DV -3.5) with a motorized injector (Stoelting) at a rate of 0.1 µL per minute. After remaining in place for 15 additional minutes, the syringe was slowly retracted. Atropine (1 mg/kg) was administered during anesthesia, and post-surgery analgesia was provided with benamine (2.5 mg/kg). Mice recovered in their home cages for at least one week before experimental manipulation.

Viral targeting for monosynaptic circuit tracing. Viral constructs were purchased from the University of North Carolina Vector Core (AAV8-EF1a-FLEX-TVA-mCherry, Addgene #38044; AAV8-CA-FLEX-RG, Addgene #38043; Watabe-Uchida et al., 2012) and the Salk Institute Gene Transfer, Targeting, and Therapeutics Core (EnvA G-deleted Rabies-eGFP, Addgene #32635; Wickersham et al., 2010). Stereotaxic surgeries were conducted at 5 months of age as described above. Unilateral basolateral amygdala injections of AAV8-EF1a-FLEX-TVA-mCherry and AAV8-CA-FLEX-RG (1:1 ratio) were

conducted three weeks prior to EnvA G-deleted Rabies-eGFP, and animals were sacrificed by transcardial perfusion one week later.

Immunofluorescence staining. Mice were deeply anesthetized with a mixture of ketamine/xylazine prior to transcardial perfusion with phosphate buffered saline (PBS) and 4% paraformaldehyde (PFA). Brains were postfixed overnight in 4% PFA and either vibratome sectioned on the coronal plane at 50 µM or prepared for cryosectioning at 25 µM as previously described (Lucas et al., 2014). Immunofluorescence staining was conducted on floating or slide-mounted sections. Primary antibodies included mouse anti-parvalbumin (1:1000; Millipore, Billerica, MA, USA; RRID:AB_2174013), guinea pig anti-GABA (1:250; Millipore; RRID:AB_91011), rabbit anti-GFP (1:500, ThermoFisher Scientific, Waltham, MA, USA; RRID:AB_10073917), chicken anti-GFP (1:1,000, Millipore; RRID:AB_90890), and rabbit anti-RFP (1:1,000, ThermoFisher Scientific; RRID:AB_2315269). Fluorescence-conjugated secondary antibodies raised in goat were purchased from Jackson Immunoresearch (West Grove, PA, USA; RRIDs:AB_2338902, AB_2337972, AB_2337398, AB_2337926). After washes in PBS, slices were blocked with 10% goat serum for 1 hr at room temperature prior to overnight incubation with primary antibodies with 5% goat serum in 0.1% Triton-X PBS at 4°C. Following washes in PBS, slices were incubated with secondary antibodies with 5% goat serum in 0.1% Triton-X PBS at room temperature for 2 hr. Slices were washed in PBS, mounted onto slides (floating sections), and coverslipped with Prolong Antifade Gold with DAPI (Life Technologies, Grand Island, NY, USA). Images were captured on a Zeiss confocal microscope attached to a computer equipped with Zenn software (Carl Zeiss Microscopy, Jena, Germany). For cell counts, images were manually quantified with the ImageJ Cell Counter plugin.

Fear conditioning. Cued auditory fear conditioning was conducted in sound attenuating chambers with automated stimulus delivery software (MedAssociates, St. Albans, VT, USA). Training entailed 6 pairings of an auditory tone (CS; 2 kHz, 80 dB, 20 s) with a co-terminating scrambled footshock (US; 1 mA, 2 s). An acclimation period of 200 s in the training arena preceded the onset of cues, and CS-US pairings were separated by an 80 s inter-trial interval. Control groups included experience naïve cage mates and unpaired animals that received explicitly unpaired training (6 CS presentations followed

by 6 US presentations in discrete sessions separated by a 15 min interval in a home cage). Mice were sacrificed 24 hours after training for slice electrophysiology.

Slice electrophysiology. Mice were anesthetized with isoflurane prior to decapitation and brain removal. Acute coronal slices of the basolateral amygdala were sectioned at 350 µm on a VT1200S vibratome (Leica Microsystems, Buffalo Grove, IL, USA) in sucrose dissection solution (in mM: 210.3 sucrose, 26.2$NaHCO_3$, 11 glucose, 4 $MgCl_2$, 2.5 KCl, 1 NaH_2PO_4, 0.5 ascorbate, and 0.5 $CaCl_2$) chilled to -4°C. Slices were recovered in standard ACSF (in mM: 119 NaCl, 26.2 $NaHCO_3$, 11 glucose, 2.5 KCl, 2 $CaCl_2$, 2 MgCl2, and 1 NaH_2PO_4) for 40 min at 34°C, then maintained at room temperature for the remainder of the experiment. All solutions were continuously bubbled with 95% O_2:5% CO_2. Whole-cell recordings were obtained with borosilicate glass electrodes (resistance: 3-5 MΩ for principal neurons, 5-8 MΩ for INs) filled with voltage clamp (in mM: 120 Cs-methanesulfonate, 10 HEPES, 10 Na-phosphocreatine, 8 NaCl, 5 TEA-Cl, 4 Mg-ATP, 1 QX-314, 0.5 EGTA, and 0.4 Na-GTP), low-chloride voltage clamp (voltage clamp without TEA-Cl), and current clamp (in mM: 127.5 K-methanesulfonate, 10 HEPES, 5 KCl, 5 Na-phosphocreatine, 2 $MgCl_2$, 2 Mg-ATP, 0.6 EGTA, and 0.3 Na-GTP) internal solutions (pH 7.25; 285-300 mOsm).

Cells were visualized on an upright DIC microscope equipped with objective-coupled LEDs (460 nm and broad spectrum (white); Prizmatix, Givat-Shmuel, Israel) for the identification of fluorescence-labeled cells as well as optogenetic cellular manipulations. Principal excitatory neurons were selected based on pyramidal morphology under DIC microscopy; recordings were terminated if physiology was inconsistent with principal cells, namely capacitance less than 120 pF and fast excitatory postsynaptic current kinetics. Electrically-evoked postsynaptic currents were obtained by stimulation of the external (cortical pathway) or internal (subcortical pathway) capsule with a matrix or concentric bipolar electrode. Monosynaptic excitatory and disynaptic inhibitory postsynaptic currents in PNs and PV-INs were isolated by holding cells at -70 mV and 0mV, respectively; compound postsynaptic currents were obtained by holding cells at -50 mV. Paired pulse ratios (PPRs) and spontaneous postsynaptic currents were obtained in picrotoxin (100 µM) for isolation of excitatory currents and in CPP (10 µM; 3-((*R*)-2-Carboxypiperazin-4-yl)-propyl-1-phosphonic acid)

and CNQX (10 μM; 6-cyano-7-nitroquinoxaline-2,3-dione) for isolation of inhibitory currents. Miniature postsynaptic currents were further isolated with tetrodotoxin (0.5 μM). Light-evoked stimulation of excitatory ChR2+ terminals evoked large polysynaptic excitatory currents in PV-INs, likely the result of feedback excitatory connections. For these experiments, saturating CPP (10 μM) and subsaturating CNQX (1 μM) was utilized to limit network excitability and thereby prevent the contamination of monosynaptic recordings with multisynaptic currents. These experiments were conducted with a low chloride cesium internal solution, which allowed for isolation of glutamatergic responses by holding the cell at -60 mV. Intrinsic excitability of PV-INs was determined by eliciting action potentials with increasing current injections (50-500 pA by 50 pA) from a resting potential of -70 mV; rheobase current was defined as the amount of current required for the generation of one action potential. The location of all cells within the basolateral amygdala was visually confirmed after recording. Data were low-pass filtered at 3 kHz (evoked) and 10 kHz (spontaneous, miniature) and acquired at 10 kHz using Multiclamp 700B and pClamp 10 (Molecular Devices, Sunnyvale, CA, USA). Evoked data were analyzed in Clampfit 10 (Molecular Devices); spontaneous and miniature currents were analyzed with MiniAnalysis (Synaptosoft, Fort Lee, NJ, USA). All data analyses were conducted blind to the experimental group.

Morphological Analysis. Live brain sections were prepared as for slice electrophysiology (see above). PV-INs were identified by tdTomato reporter expression, patched, and filled with 0.5% biocytin in voltage clamp internal solution. The location of cells within the basolateral amygdala was visually confirmed after filling. Brain slices were fixed in 4% PFA for 24 – 72 hours and stained with Alexa Flour 488-conjugated streptavidin (Johnson Immunoresearch; RRID:AB_2337249). Cells were traced on Axiophot 2 (Zeiss Microscopy, Jena, Germany) with a 40x oil immersion objective, using the Neurolucida (MBF Bioscience, Williston, VT, SA) continuous contour tracing function. The soma was traced first, using the cell body function at its brightest and most focal point. A reference point was also made at this z-level and dictated as 0.00 Z. Dendrites were traced next, using the fine focus to trace through the z-axis. Bifurcation nodes were inserted to indicate branch points in the dendritic trees. Endings were indicated as normal or incomplete; incomplete endings are indicative of truncated dendrites. Analysis was

conducted using the branched structure analysis function of Neurolucida Explorer to obtain cell perimeter data and a neuron summary, including number of dendrites, nodes, and endings.

Statistics. All statistical analyses were conducted with SPSS 20 (IBM, Armonk, NY, USA) or GraphPad Prism 5 (La Jolla, CA, USA). Two-tail paired t-tests (one group), two-tail independent samples t-tests (two groups), one-way ANOVA (≥ 3 groups), two-way ANOVA (≥ 2 groups with ≥ 2 variables), or two-way repeated-measured ANOVA (≥ 2 groups with repeating variable) were implemented to determine statistical significance. Equivalent non-parametric tests were conducted on data sets that violated assumptions of normality. All posthoc tests were chosen to maintain family wise error rate at 0.05. Data are presented as mean ± standard error of the mean (SEM) with *n* as the number of cells followed by the number of animals in parentheses.

References.

Lucas, E.K., Jegarl, A., and Clem, R.L. (2014). Mice lacking TrkB in parvalbumin-positive cells exhibit sexually dimorphic behavioral phenotypes. Behav. Brain Res. *274*, 219-225.

Watabe-Uchida, M., Zhu, L., Ogawa, S.K., Vamanrao, A., and Uchida, N. (2012). Whole-brain mapping of direct inputs to midbrain dopamine neurons. Neuron *74*, 858-873.

Wickersham, I.R., Lyon, D.C., Barnard, R.J., Mori, T., Finke, S., Conzelmann, K.K., Young, J.A., and Callaway, E.M. (2007). Monosynaptic restriction of transsynaptic tracing from single, genetically targeted neurons. Neuron *53*, 639-647.